Proceedings of the ASME 2010 29th International Conference on Ocean, Offshore and Arctic Engineering
OMAE2010
June 6-11, 2010, Shanghai, China

OMAE2010-20882

MULTI-SCALE MODELING OF WIND-WAVE INTERACTION IN THE PRESENCE OF OFFSHORE STRUCTURES FOR RENEWABLE ENERGY APPLICATIONS

Yi Liu, Di Yang, Xin Guo, and Lian Shen*
Department of Civil Engineering
The Johns Hopkins University
Baltimore, Maryland 21218
Email: lianshen@jhu.edu

ABSTRACT

We develop a multi-scale modeling capability for the simulation of wind and wave coupling dynamics, with a focus on providing environmental input for wind and wave loads on offshore structures. For the large-scale wind–wave environment, large-eddy simulation for the wind turbulence and high-order spectral simulation for the nonlinear ocean waves are dynamically coupled. For the local-scale air and water flows past the structure, we use a hybrid interface capturing and immersed boundary method. Coupled level-set/volume-of-fluid/ghost-fluid method is used to capture the wave surface. Immersed boundary method is used to represent the structure. The large-scale wind–wave simulation provides inflow boundary conditions for the local-scale air–water–structure simulation. Our simulation captures the dynamic evolution of ocean nonlinear wavefield under the wind action. The wind field is found to be strongly coupled with the surface waves and the wind load on a surface-piercing object is largely wave-phase dependent.

INTRODUCTION

To address the increasing demand of energy and the issue of global warming associated with the use of fossil fuel, clean and renewable energy is being actively seeked. The oceans provide enormous resources for renewable energy. In addition to the wave energy, the offshore wind power possesses many advantages over the traditional wind power on land and has become a new frontier in wind energy. According to a report of US Department of Energy [1], wind energy will provide 20% electricity of US demand by 2030 and 18% of them will be the offshore wind energy. Compared to the wind energy on land, the offshore wind energy is stronger and more stable, and the convenience is sea transportation makes the installation of very large wind turbine feasible. For the development of wind and wave energy technologies, there is a critical need for the understanding and modeling of ocean wind-waves, the lower part of marine atmospheric boundary layer at various sea states, and wind load and wave load on offshore structures.

A lot of efforts have been devoted to explore the physics in the marine atmospheric boundary layer and ocean boundary layer [2–4], but the complex air–sea interaction problem is still far from being solved. Complex sea condition makes the field measurement challenging and expensive. Most of the existing numerical simulations focus either on large-scale flow or on local-scale flow–structure interaction with simple boundary conditions to approximate wind and wave environment. Simulation of the interaction among wind, wave, and structure with realistic environment input is challenging because of the scale difference.

In this paper, we introduce a multi-scale modeling approach developed for the simulation of wind and wave coupling dynamics and the simulation of wind and wave past a surface-piercing object. Preliminary results of large-scale wind over broadband waves and local-scale wind–wave–structure interaction are given, which show the wave effect on the atmospheric boundary layer and the wind load on the structure.

*Address all correspondence to this author.

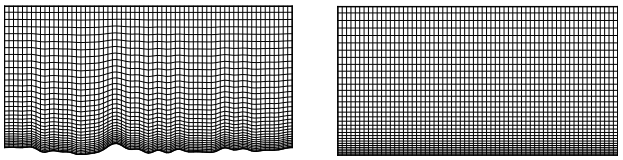

(a) (b)

Figure 1. (a) BOUNDARY-FITTED GRID IN PHYSIC SPACE. (b) CORRESPONDING CARTESIAN GRID IN COMPUTATIONAL SPACE.

NUMERICAL METHOD

Multi-scale wind–wave–structure simulation approach is developed. In this approach, the large-scale wind–wave simulation is implemented through a two-way dynamically coupled large-eddy simulation and high-order spectral method. The local-scale wind–wave–structure simulation is implemented through a hybrid interface capturing and immersed boundary method. The large-scale simulation data provides inflow condition to the local-scale simulation.

Large-Scale Wind–Wave Simulation

In the large-scale turbulent wind simulation, the non-rectangular physical domain is mapped to a rectangular computational domain with boundary fitted grid as shown in Fig. 1. The filtered Navier–Stokes equations

$$\frac{\partial \bar{\mathbf{u}}}{\partial t} + \bar{\mathbf{u}} \cdot \nabla \bar{\mathbf{u}} = -\frac{\nabla \bar{p}}{\rho_a} + \frac{\nabla \cdot \tau_{SGS}}{\rho_a} + \mathbf{g} \tag{1}$$

and

$$\nabla \cdot \bar{\mathbf{u}} = 0 \tag{2}$$

are solved on the boundary fitted grid. Here $\bar{\mathbf{u}}$ is the filtered velocity vector; t is the time; $\bar{p}$ is the filtered pressure; τ_{SGS} is the sub-grid scale stress; ρ_a is the density of the air; and $\mathbf{g}$ is the gravity acceleration. In horizontal directions, spectral method is used to achieve high order accuracy. Fast Fourier transform is used to increase the speed of computation. In the vertical direction, second-order finite difference is used. Staggered grid is used vertically. Time integration of nonlinear terms is implemented by a second-order Adams–Bashforth scheme. The Crank–Nicholson scheme is used for the viscous term. The details are referred to Yang & Shen [5].

The nonlinear surface wave simulation is implemented by the high order spectral (HOS) method [6]. In HOS, the surface elevation η and surface potential $\Phi^S(\vec{x},t) = \Phi(\vec{x},\eta,t)$ are the primary variables to be solved. The following equations,

$$\eta_t + \nabla_h \Phi^S \cdot \nabla_h \eta - (1 + \nabla_h \eta \cdot \nabla_h \eta)\Phi_z = 0 \tag{3}$$

and

$$\Phi^S_t + g\eta + \frac{1}{2}\nabla_h \Phi^S \cdot \nabla_h \Phi^S - \frac{1}{2}(1 + \nabla_h \eta \cdot \nabla_h \eta)\Phi_z^2 + p/\rho_w = 0, \tag{4}$$

derived from the kinematic and dynamic free surface boundary conditions, are solved in HOS. Here Φ is the velocity potential; Φ_z is the vertical velocity at the wave surface and it can be expressed in terms of a serial of eigenfunctions as

$$\Phi_z(\vec{x},\eta,t) = \sum_{m=1}^{M} \sum_{l=0}^{M-m} \frac{\eta^l}{l!} \sum_{n=1}^{N} \Phi_n^{(m)}(t) \frac{\partial^{l+1}}{\partial z^{l+1}} \Psi_n(\vec{x},z)|_{z=0}. \tag{5}$$

Here $\vec{x}$ represents the horizontal coordinates; ∇_h represents the horizontal gradients; p is the wind pressure; ρ_w is the water density; $\Psi_n(\vec{x},z)$ is the basis function of the n^{th} eigenmode; and $\Phi_n^{(m)}$ is the n^{th} eigenmode coefficient of the m-order perturbation potential.

The wind and wave simulations are dynamically coupled. The large-eddy simulation of wind provides pressure input to HOS. And the wave simulation by HOS evolves in time and provides new bottom boundary conditions to the wind simulation.

Local-Scale Wind–Wave–Structure Simulation

At the local-scale, we use coupled level-set/volume-of-fluid/ghost-fluid method on Cartesian grid to capture the air–water interface. Level set method uses the signed distance function

$$\phi(\vec{x}) = \begin{cases} d & water \\ 0 & interface \\ -d & air \end{cases} \tag{6}$$

to represent the interface. Here d is the distance to the interface. The motion of the interface is governed by the Lagrangian-invariant level-set transport equation

$$\frac{\partial \phi}{\partial t} + \vec{u} \cdot \nabla \phi = 0. \tag{7}$$

This transport equation does not guarantee the level set function ϕ to be a signed distance function in the process of time integration. So the reinitialization equation

$$\frac{\partial d}{\partial \tau} + sign(\phi)(|\nabla d| - 1) = 0 \tag{8}$$

is used to correct ϕ for it to remain as the signed distance function [7, 8]. Here τ is an artificial time; initial condition is $d(\vec{x},0) =$

$\phi(\vec{x})$; and $\phi(\vec{x})$ is replaced by $d(\vec{x},\tau_{steady})$ after Eqn. 8 is solved to steady state.

The ghost fluid method (GFM) is used to have sharp interface and avoid spurious current [9]. In GFM, the interface jump condition

$$\left[\begin{pmatrix}\mathbf{N}\\ \mathbf{T}_1\\ \mathbf{T}_2\end{pmatrix}(p\mathbf{I}-\tau)\mathbf{N}^T\right]=\begin{pmatrix}\sigma\kappa\\ 0\\ 0\end{pmatrix} \tag{9}$$

is addressed explicitly in the calculation of the stress and the pressure Poisson equation with subcell resolution [10]. Here $\mathbf{N},\mathbf{T}_1,\mathbf{T}_2$ are the unit normal vector and the two orthogonal unit tangential vectors of the interface, respectively; p is the pressure; τ is the viscous stress tensor; $\mathbf{I}$ is the identity matrix; σ is the surface tension coefficient; and κ is the surface curvature.

The volume of fluid (VOF) method is coupled with the level set method to improve the mass conservation. The VOF equation is solved simultaneous with the level set equation. Level set function provides the surface normal to VOF surface reconstruction and VOF provides the volume information to correct the level set function [11].

The immersed boundary method (IBM) is used to simulate the flow–structure interaction on the Cartesian grid [12]. In IBM, a body force is introduced into the momentum equation to account for the presence of the structure. The momentum equation is modified by the addition of a force term as

$$\frac{\partial \mathbf{u}}{\partial t}=\mathbf{RHS}+\mathbf{f}. \tag{10}$$

The force $\mathbf{f}$ is calculated according to the known velocity of the structure from the discretized equation directly.

Multi-Scale Simulation

Uniform inflow boundary condition is widely used in existing simulations of flow–structure interaction. For the environmental wind and wave inputs to be included, large-scale and local-scale simulations are combined together for a multi-scale wind–wave–structure simulation. A subdomain of the large-scale simulation data is extracted and used by the local-scale simulation as the inflow boundary condition. This process is displayed in Fig. 2.

RESULTS

In Fig. 2, the large-scale wind–wave simulation result of turbulent wind over complex broadband wave field is presented on the left. The wave age c/u^* defined as the ratio between the phase speed of the dominant wave c and the turbulence friction

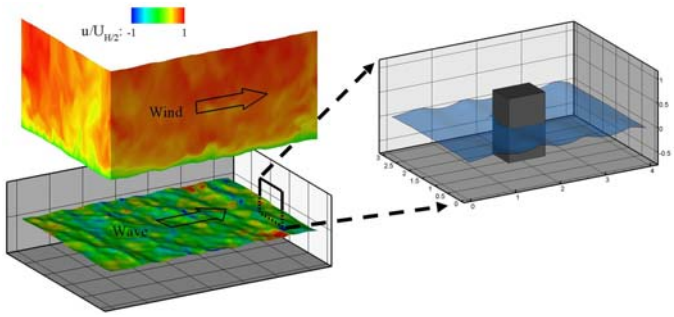

Figure 2. ILLUSTRATION OF MULTI-SCALE WIND–WAVE–STRUCTURE SIMULATION. AIR DOMAIN OF LARGE-SCALE SIMULATION IS LIFTED UP FOR BETTER VISUALIZATION. PRESSURE ON THE SURFACE OF WAVES IS SHOWN. THE FLOW CONDITION INSIDE THE SMALL BLACK WINDOW IS PROVIDED TO LOCAL SCALE WIND–WAVE–STRUCTURE SIMULATION AS INFLOW CONDITION.

velocity u^* is 2. The air domain with streamwise wind velocity contours is lifted up for better visualization. The pressure field on the water surface shows that the windward pressure is larger than the leeward pressure statistically. The pressure difference provides forcing for the wave growth.

In Fig. 3, the local-scale wind–wave–structure simulation results at two different wave phases are presented. Vertical streamwise velocity, surface elevation, and pressure on the object surface are plotted. Complex vortical structures in the wake of the surface piercing object are shown. Strong wave-coherent flow patterns near the water surface are seen. In Fig. 4, the enlarged wind velocity contours above the wave crest and trough are presented. Above the wave crest, the wind shear is strong and the wind velocity is large. Above the wave trough, the wind velocity is small because of the sheltering effect behind the wave crest. When a wave crest arrives at the front surface of the object, the pressure on it is obviously larger than that when a wave trough arrives. The wind drag coefficients are calculated and the difference is found to be 24%. The phase dependence of wind load could severely affect the energy input to wind turbines and could also incur structural vibration and damage.

CONCLUSION

In this study, we develop a multi-scale wind–wave–structure simulation approach. This approach combines large-scale environmental wind–wave simulation and local-scale wind–wave–structure simulation, and may provide data for offshore wind energy applications.

Our simulation results show that the wind flow in the atmospherical boundary layer is highly wave phase dependent, which

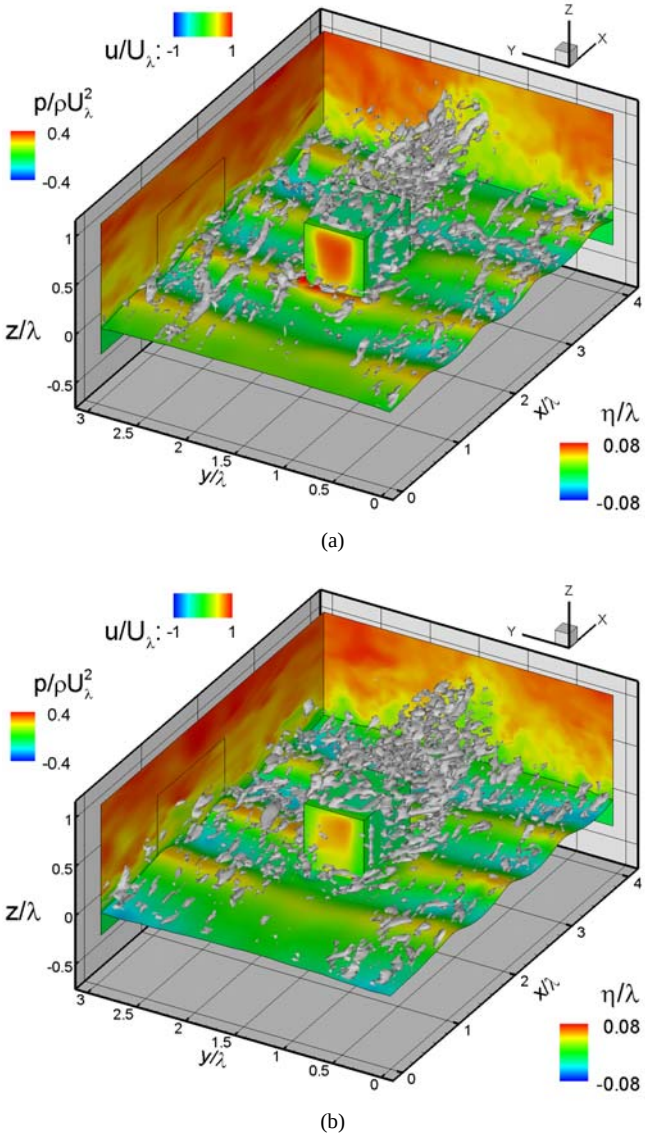

Figure 3. WIND AND WAVE FIELDS AROUND A SURFACE PIECING BODY: (a) WHEN A WAVE CREST, AND (b) WHEN A WAVE TROUGH ARRIVES AT THE FRONT SURFACE OF THE OBJECT. THE INFLOW IS IN THE X-DIRECTION. THE VERTICAL PLANES SHOW THE STREAMWISE VELOCITY CONTOURS. THE VELOCITY FIELD INSIDE THE SMALL BLACK WINDOW IS ENLARGED AND SHOWN IN FIG. 4. THE PRESSURE ON THE OBJECT SURFACE AND THE WAVE SURFACE ARE SHOWN. VORTICES ARE PLOTTED WITH GREY COLOR.

makes the wind drag on surface-piercing structure also wave phase dependent. For turbine efficiency and structure stability, it may be necessary to consider the coupling dynamics of wind, wave, and structure.

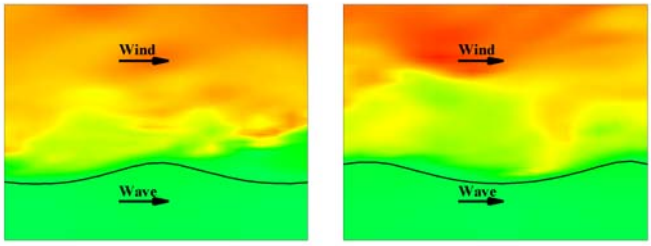

Figure 4. ENLARGED STREAMWISE VELOCITY CONTOURS FROM FIG. 3: (a) ABOVE WAVE CREST WHEN A CREST ARRIVES AT THE OBJECT; (b) ABOVE WAVE TROUGH WHEN A TROUGH ARRIVES AT THE OBJECT.

REFERENCES

[1] Lindenberg, S., Smith, B., O'Dell, K., and et al, 2008. 20% wind energy by 2030: increasing wind energy's contribution to u.s. electricity supply. Tech. rep., Department of Energy, July. See also URL `http://www.eere.energy.gov/windandhydro`.

[2] Komen, G. J., Cavaleri, L., Donelan, M., Hasselmann, K., Hasselmann, S., and Janssen, P. A. E. M., 1994. *Dynamics and modelling of ocean waves*. Cambridge Univ. Press, Cambridge, UK.

[3] Janssen, P., 2004. *The interaction of ocean waves and wind*. Cambridge Univ. Press, Cambridge, UK.

[4] Csanady, G. T., 2001. *Air–sea interaction: Laws and Mechanisms*. Cambridge Univ. Press, Cambridge, UK.

[5] Yang, D., and Shen, L. "Direct simulation based study of turbulent flow over various waving boundaries". *J. Fluid Mech.(in press)*.

[6] Dommermuth, D. G., and Yue, D. K. P., 1987. "A high-order spectral method for the study of nonlinear gravity waves". *J. Fluid Mech.*, ***184***, pp. 267–288.

[7] Sussman, M., Smereka, P., and Osher, S., 1994. "A level set approach for computing solutions to incompressible two-phase flow". *J. Comput. Phys.*, ***114***, pp. 146–159.

[8] Sussman, M., Fatemi, E., Smereka, P., and Osher, S., 1998. "An improved level set method for incompressible two-phase flows". *Computers & Fluids*, ***27***(5-6), pp. 663–680.

[9] Kang, M., Fedkiw, R. P., and Liu, X., 2000. "A boundary condition capturing method for multiphase incompressible flow". *J. Sci. Comput.*, ***15***(3), pp. 323–360.

[10] Liu, X., Fedkiw, R. P., and Kang, M., 2000. "A boundary condition capturing method for poisson's equation on irregular domain". *J. Comput. Phys.*, ***160***, pp. 151–178.

[11] Sussman, M., and Puckett, E. G., 2000. "A coupled level set and volume-of-fluid method for computing 3d and axisymmetric incompressible two-phase flows". *J. Comput.*

Phys., ***162***, pp. 301–337.
[12] Mittal, R., and Iaccarino, G., 2005. "Immersed boundary method". *Annu. Rev. Fluid Mech.,* ***37***, pp. 239–261.